J. Membrane Biol. 212, 61–68 (2006)
DOI: 10.1007/s00232-006-0003-8

The Journal of
Membrane
Biology

Permeability Changes of *Manduca sexta* Midgut Brush Border Membranes Induced by Oligomeric Structures of Different Cry Toxins

C. Muñoz-Garay[1], J. Sánchez[1], A. Darszon[1], R.A. de Maagd[2], P. Bakker[2], M. Soberón[1], A. Bravo[1]
[1]Instituto de Biotecnología, Universidad Nacional Autónoma de México, Apdo postal 510-3, Cuernavaca, Morelos 62250, México
[2]Plant Research International, P.O. Box 16, 6700 AA Wageningen, The Netherlands

Received: 12 January 2006/Accepted: 9 June 2006

Abstract. The pore-formation activity of monomeric and oligomeric forms of different Cry1 toxins (from Cry1A to Cry1G) was analyzed by monitoring ionic permeability across *Manduca sexta* brush border membrane vesicles. The membrane vesicles were isolated from microvilli structures, showing a high enrichment of apical membrane markers and low intrinsic K^+ permeability. A fluorometric assay performed with 3,3′-dipropylthiodicarbocyanine fluorescent probe, sensitive to changes in membrane potential, was used. Previously, it was suggested that fluorescence determinations with this dye could be strongly influenced by the pH, osmolarity and ionic strength of the medium. Therefore, we evaluated these parameters in control experiments using the K^+-selective ionophore valinomycin. We show here that under specific ionic conditions changes in fluorescence can be correlated with ionic permeability without effects on osmolarity or ionic strength of the medium. It is extremely important to attenuate the background response due to surface membrane potential and the participation of the endogenous permeability of the membrane vesicles. Under these conditions, we analyzed the pore-formation activity induced by monomeric and oligomeric structures of different Cry1 toxins. The Cry1 toxin samples containing oligomeric structures correlated with high pore activity, in contrast to monomeric samples that showed marginal pore-formation activity, supporting the hypothesis that oligomer formation is a necessary step in the mechanism of action of Cry toxins.

Key words: *Bacillus thuringiensis* — Pore-forming toxin — *Manduca sexta* — Membrane potential — $diSC_3(5)$ — Oligomeric Cry toxin

Correspondence to: A. Bravo; email: bravo@ibt.unam.mx

Introduction

The Cry toxins found in different *Bacillus thuringiensis* (Bt) strains cause mortality to susceptible insects by lysing the midgut epithelium cells [1, 2]. In order to exert their toxic effect, a transition from crystal inclusion protoxins to membrane-inserted pores is required. In the case of the Cry1A toxins, it was reported that they interact sequentially with two protein receptors located in the apical membrane of *Manduca sexta* larvae midgut cells [3, 4]. The interaction of the monomeric Cry1A with the cadherin receptor induces toxin oligomerization [4, 5]. The oligomerization of Cry1A toxin increases its affinity to the second receptor, aminopeptidase-N. Aminopeptidase-N localizes the toxin in membrane microdomains, where it is inserted and induces the formation of ionic pores [4, 6]. These ionic pores shunt the potential difference gradient and disrupt the K^+ and H^+ gradients, affecting nutritional uptake with eventual lysis of the midgut cells [2]. It was proposed that the oligomeric structure of Cry1A toxin is an intermediary in the process of membrane insertion; it is defined as pre-pore since it is formed outside of the membrane after interacting with cadherin and the cleavage of helix α-1 [5]. The pre-pore is an insertion-competent structure that produces stable channels in black lipid bilayers with high open probability in contrast to the monomeric structure [7]. The structural changes of Cry toxins during oligomerization and insertion into the membrane are not known. The Cry1Ab pre-pore is soluble at low concentrations, displays new hydrophobic surfaces with respect to the monomeric form and is highly resistant to heat denaturalization [8]. However, the formation of Cry oligomeric structures has been demonstrated only for Cry1Ab and Cry3 toxins [5, 7, 9]. In this work, we analyzed the oligomer formation of different Cry1 toxins and correlated the presence of their oligomeric structures with high pore-formation activity.

Different approaches have been used in the study of the pore activity of Cry toxins. We have routinely used a fluorescent dye sensitive to changes in membrane potential, 3,3′-dipropylthiodicarbocyanine iodide ($diSC_3$[5]) [5, 8, 10, 11]. Fluorescent probes that sense transmembrane potential differences [12] have been extensively used to detect rapid changes in membrane potential of cells, organelles and vesicles [13]. The sensitivity of the cyanine dye $diSC_3(5)$ to membrane voltage depends on the fact that it has a delocalized positive charge and behaves as a permeant cation. The membrane potential drives its distribution between the inside of the vesicles and the medium. When the vesicles are hyperpolarized, the dye is accumulated in the vesicle and its fluorescence is quenched due to the formation of dye aggregates [14]. The response time of the measurement is short [12, 13], and changes in fluorescence level are directly associated to changes in membrane potential induced by the changes in ionic flux. However, the use of this system to determine pore formation by Cry toxins has been questioned [15]. Here, we validated the use of $diSC_3(5)$, showing that under specific ionic conditions, where the surface membrane potential is shielded and the intrinsic permeability is inhibited, the ionic strength and osmolarity have no effects on the analysis of membrane potential of *M. sexta* membrane vesicles and changes in fluorescence can be correlated with ionic permeability induced by Cry toxins.

Our data show that the oligomeric structure of different Cry1 toxins works like a permeant pore, where the ions move as a function of the electrochemical gradient through the toxin pore, changing the membrane potential of the vesicle. The monomeric toxins showed a marginal effect, confirming that the oligomeric structure of Cry toxins is the intermediate responsible for insertion into the membrane.

Materials and Methods

Preparation of Brush Border Membrane Vesicles

Brush border membrane vesicles (BBMVs) were prepared from isolated microvilli structures purified from midgut tissue of *M. sexta* fourth instar larvae [16]. Briefly, the midgut epithelium cells were dissociated by 1-h incubation of the midgut tissue in 100 ml phosphate-buffered saline (PBS) supplemented with 5 mM ethylenediaminetetraacetic acid (EDTA), 5 mM ethyleneglycoltetraacetic acid (EGTA), 1 mM phenylmethyl sulfonyl fluoride (PMSF) and 100 μg/ml leupeptin. Cells were collected by centrifugation for 5 min at 120 × *g* and washed three times with PBS. Isolated cells were homogenized by gentle mechanical disruption (2–4 min in vortex at maximal velocity), loaded in a 12-ml linear Percoll density gradient (10–35%; Sigma, St. Louis MO) in PBS and centrifuged for 10 min at 2,500 × *g* in a swing rotor (5804R; Eppendorf, Hamburg, Germany) at 4°C. The gradients were fractionated, and fractions containing the microvilli structures were selected by microscopy observations. The microvilli fractions were suspended in 150 mM KCl, 10 mM 4-(2-hydroxyethyl)-1-piperazineethanesulfonic acid (HEPES)-HCl (pH 7) and washed three times by centrifugation. Finally, they were sonicated for six periods of 30 sec each at 25°C (Branson 1200 Sonic Bath; Branson, Danbury, CT) in the same solution. BBMV enrichment was estimated according to the alkaline phosphatase (ALP) and aminopeptidase-N (APN) activity (22- and 35-fold increase/mg protein, respectively) relative to the initial homogenate. APN activity was assayed using L-leucine-*p*-nitroanilide as substrate [11] and APL, using *p*-nitrophenyl phosphate as substrate [17].

Preparation of Small Unilamellar Vesicles

Egg-derived phosphatidylcholine (PC) lipids from a chloroform stock (Avanti Polar Lipids, Alabaster, AL) were mixed in glass vials at 2.6 μmol total and dried by argon flow evaporation, followed by overnight storage under vacuum to remove residual chloroform. The lipids were hydrated in 2.6 ml of HEPES 10 mM, 150 mM KCl (pH 7) by a 30-min incubation period, followed by vortexing. To prepare small unilamellar vesicles (SUVs), the lipid suspension was subjected to sonication five times for 5 min in the Branson 1200 bath sonicator. Liposomes were used within 4–5 days of their preparation. Liposomes were prepared at 1 mM total lipid concentration and diluted to the required concentration just before use.

Preparation of Insecticidal Crystal Proteins

Cry1Ab crystals were produced in *Bt* strain 407cry^- transformed with pHT315–1Ab plasmid. Cry1Ab crystals were purified by sucrose gradients and protoxin solubilized in 50 mM Na_2CO_3 (pH 10.5), 0.2% β-mercaptoethanol at 37°C for 2 h [18]. The oligomeric and monomeric forms of Cry1Ab toxin were produced by incubating Cry protoxin for 1 h with scFv73 antibody in a mass ratio of 1:4 and digested with midgut juice (5%) for 1 h at 37°C. PMSF, 1 mM, was added to stop the reaction. Finally, the monomeric and oligomeric forms of Cry1Ab were purified by size-exclusion chromatography in a Superdex 200 HR 10/30 (Amersham Pharmacia Biotech, Uppsala, Sweden) as previously reported [7, 19].

The Cry1Aa, Cry1Ca, Cry1Da, Cry1Ea, Cry1Fa and Cry1Ga protoxins were obtained as recombinant proteins expressed in *Escherichia coli*. The inclusion bodies were solubilized and purified as described [20]. The monomeric structure of the toxins was produced by activation of protoxins with trypsin in a mass ratio of 1:20 for 1 h at 25°C. PMSF was added to a final 1 mM concentration to stop proteolysis. The oligomeric structure of these toxins was produced by incubation of 100 μg of each Cry protoxin for 15 min at 25°C with 10 μg of BBMV isolated from *M. sexta* midgut tissue in the absence of protease inhibitors; the reaction was stopped with 1 mM PMSF, and samples were centrifuged (20 min at 12,000 x *g*) [5, 9]. Protein concentration was determined in the supernatant by Bradford assay using bovine serum albumin as standard.

Fluorescence Measurements

Electrical potential differences were measured using the positively charged potential-sensitive dye $diS\text{-}C_3$-(5) (Molecular Probes, Eugene, OR). Fluorescence was recorded at the 620/670 nm excitation/emission wavelength pair using an Aminco Bowman (Urbana, IL) luminescence spectrometer as in [10]. Stock dye solution, 0.5 μl (1 mM in dimethyl sulfoxide), was added to 0.9 ml of buffer solution (150 mM tetramethylammonium chloride [TMA-Cl], 2 mM $CaCl_2$,10 mM HEPES [pH 7]) in a 1-cm path

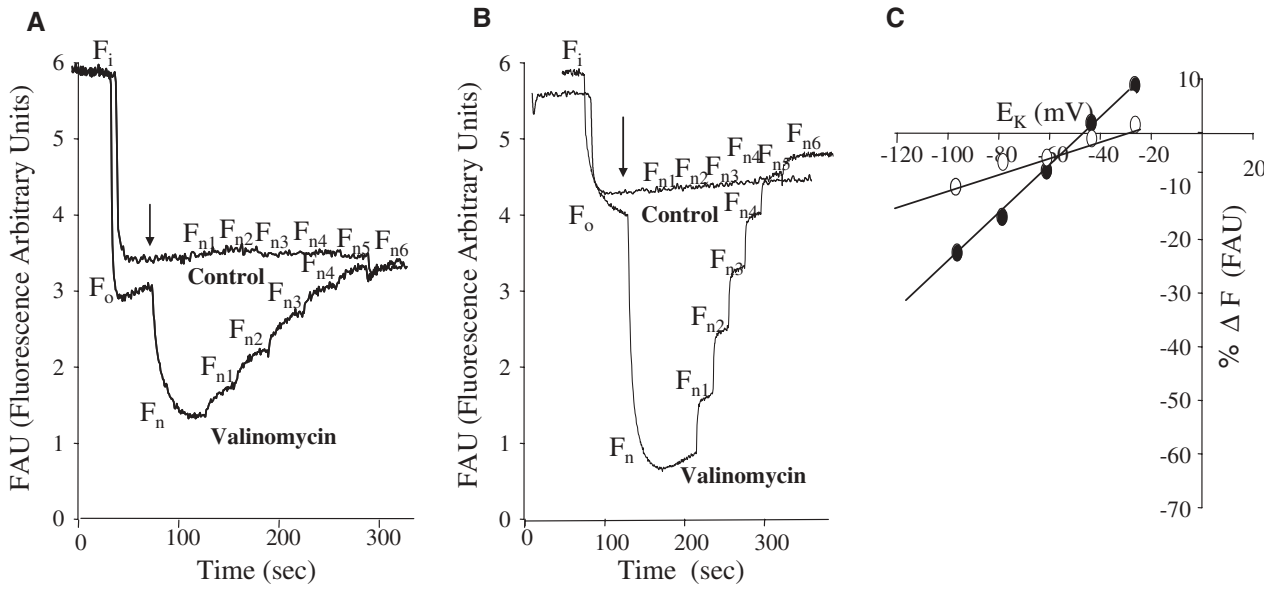

Fig. 1. K^+-diffusion potential induced by valinomycin. Fluorescence response induced by 0.1 μM valinomycin in BBMVs isolated from *M. sexta* larvae (*A*) or in SUV liposomes (*B*) suspended in 150 mM TMA^+, 2 mM $CaCl_2$ (pH 7.0). The fluorescent dye $diSC_3(5)$ was used at 0.2 μM, and the successive additions of KCl (F_{n1}–F_{n6}) were 1, 2.5, 6, 12.5, 26 and 52 mM final concentration, respectively. The resting membrane potential was estimated from the curve of the percentage of changes in fluorescence arbitrary units (% Δ FAU) vs. K^+ equilibrium potential (E_K, in m*V*) (*C*). White circles, BBMVs; black circles, SUVs.

length cuvette, and the maximal initial fluorescence (F_i) was measured (Fig. 1A). For some experiments, TMA-Cl was substituted with 150 mM methylglucamine chloride (MeGluCl), NaCl or KCl, as indicated in the text. BBMVs (10 μg) or SUVs (15 μM) previously loaded with 150 mM KCl as described above were added (F_o). All determinations were made at 25°C with constant stirring.

Dye calibration and determination of resting membrane potential were performed in the presence of valinomycin (0.1 μM) by successive additions of KCl (F_{n1} = 1, F_{n2} = 2.5, F_{n3} = 6, F_{n4} = 12.5, F_{n5} = 26, F_{n6} = 52, mM final concentration). The changes in fluorescence were normalized as percentage of changes in fluorescense arbitrary units

(% Δ FAU) = $[(F_n - F_o)/F_i] \times 100$, where F_n is the FAU at the different KCl calibrations and F_o is the FAU at the equilibrium obtained after BBMV or SUV addition to the dye in solution. The % Δ FAU vs. K^+ equilibrium potential (E_K in m*V*) was determined, and the slope (*m*) of this curve is directly correlated with the permeability. The E_K was calculated with the Nernst equation. Changes in fluorescence determinations were done at least four times.

Insects Bioassay

Bioassays were performed with *M. sexta* neonate larvae by surface contamination method [5]. Toxin solution was poured on the diet surface and allowed to dry. Neonate *M. sexta* larvae were placed on the dried surface and the mortality was monitored after 7 days.

Results

Membrane Potential Calibrations in BBMVs and in SUVs Liposomes

Valinomycin, a K^+-selective ionophore, was used to induce a K^+-diffusion potential, as given by the Nernst relation $E_K = 25.69 \ln [K^+]_{out}/[K^+]_{in}$, assuming that the K^+ conductance due to valinomycin overwhelms the intrinsic ionic conductance of the BBMV. Figure 1 shows the fluorescence response to changes in the K^+-diffusion potential by varying external K^+ concentration in the presence of valinomycin in BBMVs isolated from *M. sexta* larvae (Fig. 1A) and in SUVs (Fig. 1B) suspended in 150 mM TMA^+, 2 mM $CaCl_2$ (pH 7.0). Control traces corresponding to intrinsic permeability to KCl of the isolated BBMVs or SUVs showed no permeability in the absence of valinomycin. These control traces indicated that under these conditions the vesicles had very low intrinsic K^+ permeability and that there were no artifacts during calibration. The maximal value of traces is due to the fluorescence of the dye in solution (F_i). After BBMV or SUV addition, the dye distributes across the membrane according to the potential, achieving a stable fluorescence signal (F_o). Addition of valinomycin increases K^+ permeability, leading to efflux from the vesicles, which results in membrane hyperpolarization, inward flow of the dye and quenching of the fluorescence (F_n). Finally, successive additions of KCl (1–50 mM final concentration) generated different K^+-diffusion potentials across the vesicles. These depolarizations were produced with the consequent outward flow of the dye (F_{n1}, F_{n2}, F_{n3}, F_{n4} ...).

A bonus in the valinomycin calibration procedure is the estimation of the resting potential of the vesicles ($E_R = F_o$). When the intra-/extracellular K^+ concentrations are known, the diffusion potentials

(E_K) can be calculated by the Nernst equation. The cyanine dye response is calibrated in order to determine the external K^+ concentration at which the signal equals the F_o, known as the null point. At the null point, the K^+ concentration ratio equals the value at the resting membrane potential F_o and E_R could be calculated. The percentage changes in fluorescence were plotted against E_K (Fig. 1C); a straight line was obtained, where the intercept with the *x* axis indicates the resting membrane potential ($E_R = -30.9$ or -50 m*V* for BBMVs or SUVs, respectively). The slope is a relative measure of K^+ permeability induced by valinomycin in BBMVs ($m = 0.19$) or SUVs ($m = 0.42$).

The E_R of the BBMVs was also determined when different monovalent ions (150 mM *N*-methyl-D-glucamine [$NMDG^+$] or 150 mM Na^+) were used to replace the TMA^+ in the external solution (150 mM monovalent ion, 2 mM $CaCl_2$,10 mM HEPES [pH 7]). We found that the E_R has a similar value under these conditions (-30 ± 4 m*V*), as expected if the basal permeability of BBMVs to $NMDG^+$, TMA^+ and Na^+ were low.

It is important to determine the adequate concentrations of cyanine dye and valinomycin since the characteristics of different BBMV preparations may vary. High concentrations of cyanine (>2 μM) can induce a depolarization; the optimal cyanine concentration ranged between 0.2 and 1 μM. We determined that 0.5–1 μM valinomycin is enough to clamp the membrane potential to E_K and produce a stable fluorescent signal.

Effect of Surface Potential, Osmolarity, and Ionic Strength on Membrane Potential Determinations

Biological membranes possess fixed charges on their surface, producing a surface potential [21]. The ionic strength has an important effect on the surface potential since mobile ions in the external medium shield the exposed charge on the membrane surface [21]. In addition, since the phosphate group can be protonated depending on the pH, changes in pH can also affect surface potential by altering the ionization state of the phospholipids [21]. Figure 2 shows that in the absence of divalent cations on the external medium the fluorescent dye responded to K^+ calibrations. This response could be due to changes in surface potential or to the presence of an endogenous K^+ permeability sensitive to inhibition by $CaCl_2$ and $MgCl_2$. The successive additions of KCl could partially shield the exposed negative charges of the membrane, and the surface potential fell off, resulting in changes in the fluorescence of the dye. However, in the presence of 2 mM $CaCl_2$ or $MgCl_2$, the negative surface potential of the membrane could be shielded and the endogenous K^+ permeablility could be inhibited, resulting in a small response of the BBMVs to KCl additions (Fig. 2).

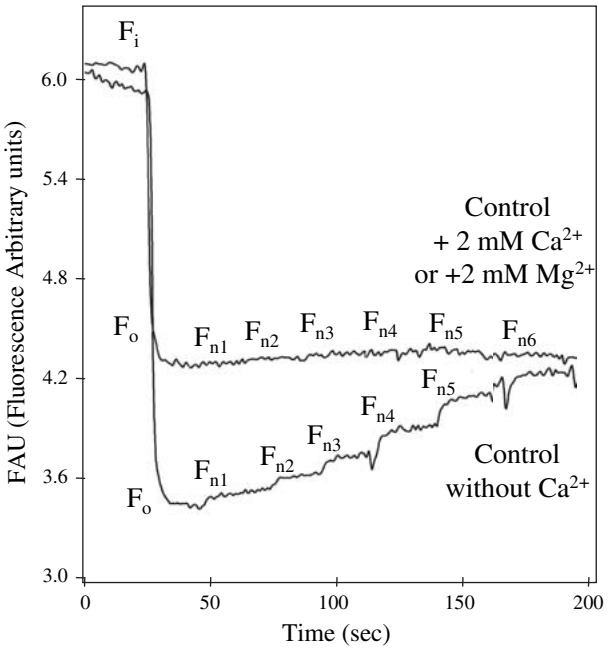

Fig. 2. Response of the fluorescent dye $diSC_3(5)$ to changes in surface potential. Conditions were similar to those in Figure 1 with the exception of valinomycin addition. Measurements in the presence of 2 mM $CaCl_2$ or 2 mM $MgCl_2$ shielded the negative surface potential of the *M. sexta* BBMVs, resulting in a stable signal after the successive KCl additions.

A previous report suggested that osmolarity and ionic strength have a dramatic effect on cyanine $diSC_3(5)$ dye sensibility and on the estimations of the changes in membrane potential [15]. In order to analyze the effect of ionic strength and osmolarity in our determinations of BBMV membrane potential, we analyzed the K^+ permeability induced by valinomycin under steady-state conditions where background response is reduced by the presence of divalent cations in the external solution. The relative K^+ permeability was determined by analyzing the slope (*m*) of the curve of % Δ FAU vs. E_K (Fig. 3A), and the resting membrane potential of the BBMVs (Fig. 3B) was determined as described above. The external solution (150 mM TMA^+, 2 mM Ca^{2+}) was supplemented with 150 mM sucrose or 150 mM NaCl in order to increase the osmolarity or the ionic strength, respectively. Figure 3A shows that the *m* values were very similar under these conditions, suggesting that the relative K^+ permeability was not affected by changes in osmolarity or in ionic strength. Similarly, no significant statistical differences were found in the estimated E_R values under these conditions (Fig. 3B).

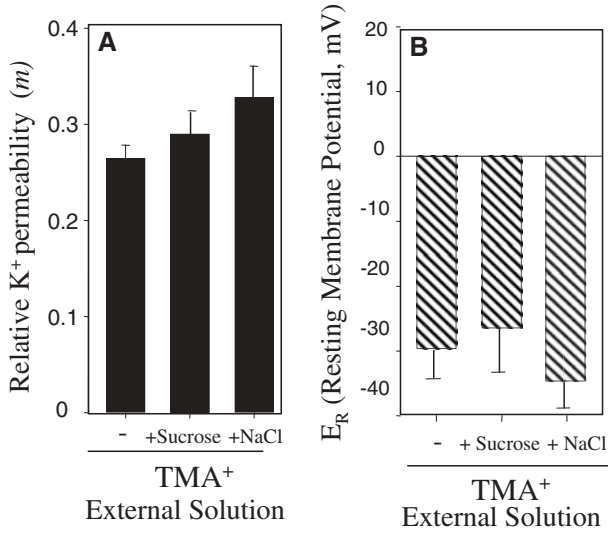

Fig. 3. Effect of ionic strength and osmolarity on the K^+ permeability induced by valinomycin in BBMVs. Relative K^+ permeability (*m*) (*A*) and resting membrane potential (E_R) (*B*) were determined by the curve of changes in fluorescence (% Δ FAU) vs. K^+ equilibrium potential (E_K). BBMVs were suspended in 150 mM TMA^+, 2 mM Ca^{2+} and supplemented with 150 mM sucrose or 150 mM NaCl as indicated.

Permeability Induced by CRY1AB Toxin in M. sexta BBMVS

Figure 4A shows a representative trace of the changes in membrane potential induced by pure Cry1Ab oligomeric toxin. Addition of 2.5 nM of the oligomeric Cry toxin to BBMVs at pH 7 produced a fast hyperpolarization. The response of the dye to KCl additions was increased when the oligomeric Cry1Ab toxin was added to the vesicles, in contrast to control traces in which the same amount of buffer or 2.5 nM monomeric Cry1Ab toxin was added. After each KCl addition, a new membrane potential was established and a depolarization produced. Figure 4B is a summary of the *m* values for each condition. The slope obtained with 0.5 nM of oligomeric Cry1Ab demonstrated that the K^+ permeability induced by Cry1Ab is dose-dependent. In addition, Figure 4B shows that the oligomeric structure has higher activity than the monomeric structure at the same concentration.

Permeability Induced by Oligomeric Structures of Different Cry1 Toxins in *M. sexta* BBMVs

M. sexta is susceptible to other Cry toxins: Cry1Aa, Cry1Ca, Cry1Da, Cry 1Ea and Cry1Fa (Table 1). We anticipated that the mechanism of action of these Cry toxins also involves the formation of an oligomeric structure that is insertion-competent. In order to analyze the oligomerization and the pore-formation activity of these toxins, pure protoxin preparations were activated by 15-min incubation with *M. sexta* BBMVs isolated in the absence of protease inhibitors at 25°C. As control, these protoxins were activated by trypsin treatment (1 h 1:20 at 25°C) (Fig. 5A). Previously, we showed that Cry1Ab protoxin activated with trypsin produced only the monomeric structure [5]. We also showed that Cry1Ab could be activated by 15-min incubation with *M. sexta* BBMVs isolated without protease inhibitors, inducing formation of the pre-pore oligomeric structure [5], suggesting the existence of proteases associated with BBMVs. Incubation with BBMVs promoted the formation of a 250-kDa oligomeric structure of all these Cry1 toxins (Fig. 5B). We analyzed the K^+ permeability induced by Cry toxin samples activated with trypsin or with *M. sexta* BBMVs at 1.4 μg protein per reaction. The samples activated with BBMVs showed formation of an oligomeric structure (Fig. 5B) and resulted in higher pore-formation activity (Fig 5C) compared with the samples activated with trypsin that contained only the monomeric structure (Fig. 5A, C). As a control, we included Cry1Ga toxin, which is not active against *M. sexta* larvae (Table 1); and it did not induce K^+ permeability in *M. sexta* membranes (Fig. 5C). Nevertheless, the oligomer formation of Cry1Ga could not be analyzed since the Cry1Ab polyclonal antibody does not react with Cry1Ga.

Discussion

The pore-formation activity of Cry toxins is an important step during insect intoxication and a cause of the cell lysis of the midgut epithelium. However, many unanswered questions remain regarding Cry pore-formation activity and the characteristics of the toxin after insertion into the membrane. Different strategies have been used to explore pore-formation activity of Cry toxins. Studies with isolated BBMVs represent a powerful tool in analyses of the cellular mechanisms involved in transmembrane transport, the interaction of Cry toxins with their receptors and their pore-formation activity. The purification of BBMVs is of key importance to avoid misleading interpretations due to contamination with other cell membranes harboring additional proteins. The intrinsic K^+ permeability observed in BBMVs may represent ionic channels that are normally present in the microvilli membrane or channels from basolateral membrane cross-contamination produced during BBMV preparation. We have developed a methodology to purify BBMVs from isolated microvilli structures rather than from whole midgut homogenate that resulted in a high enrichment of microvilli aminopeptidase (35-fold) and ALP (22-fold) and in reduced intrinsic K^+ permeability [16].

In this work, we validated the use of a fluorometric assay to analyze the changes in membrane potential produced by Cry1Ab toxin. One advantage

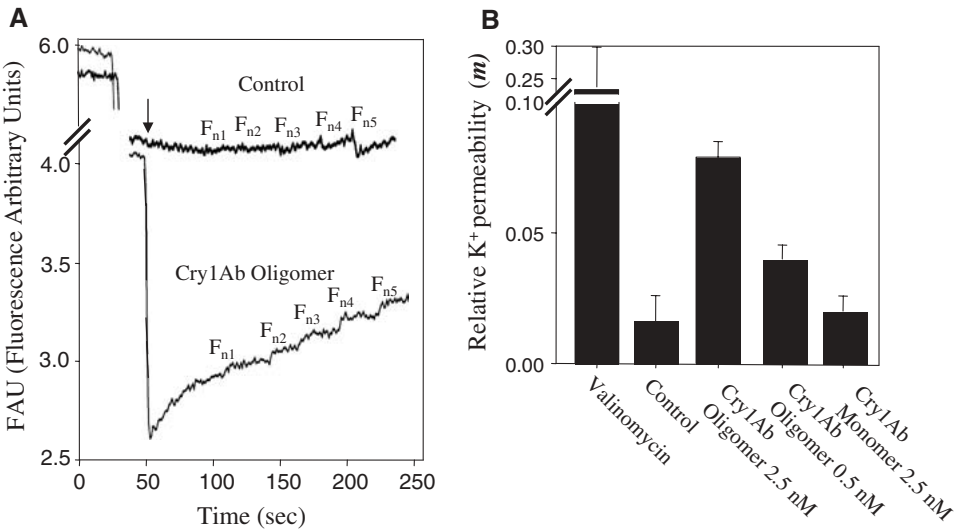

Fig. 4. Permeability induced by Cry1Ab toxin in *M. sexta* BBMVs. Representative trace of changes in membrane potential induced by 2.5 nM Cry1Ab oligomeric toxin and control trace after buffer addition (*A*) and relative K^+ permeability (*m*) (*B*) obtained with different oligomeric Cry1Ab toxin concentrations (2.5 or 0.5 nM) or Cry1Ab monomeric toxin (2.5 nM).

Table 1. Toxicity of different Cry1 proteins to *M. sexta* larvae

Toxins	LC_{50} (ng/cm^2) 50% lethal concentration
Cry1Aa	10 (6–13)[a]
Cry1Ab	2 (1–3.5)
Cry1Ca	50 (41–65)
Cry1Da	100 (87–120)
Cry1Ea	220 (180–270)
Cry1Fb	114 (89–135)
Cry1Ga	> 2,000

[a]95% fiducial limits in parentheses.

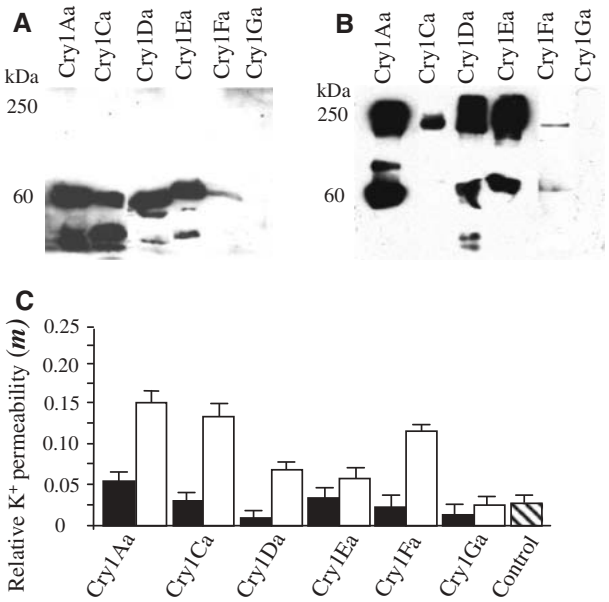

Fig. 5. Activation and pore-formation activity of different Cry1 toxins. Western blot analysis of the different Cry1 toxins activated with trypsin, showing only 60-kDa monomeric toxin and some small bands produced by toxin degradation. (*A*) Western blot of the monomeric and oligomeric structures of the different Cry1 toxins obtained after activation with *M. sexta* BBMVs. (*B*) Relative K^+ permeability (*m*) of toxin samples activated with BBMVs (white bars, 1.4 μg) and their corresponding trypsin-activated toxin (black bars, 1.4 μg) (*C*).

of the membrane potential measurements is their rapid response time and the possibility of analyzing the efficiency in the permeability of a particular ion independently of its contra-ion, an important difference when comparing with light-scattering assays that analyze the permeability of both cation and anion at the same time. We show here that for membrane potential measurements it is extremely important to screen the surface potential that most biological membranes possess due to the presence of fixed charges on their surface. We used Ca^{2+} ions to shield the surface potential of the membrane since it has been shown that surface potential is far more reduced by multivalent counterions than univalent ones [22]. In the absence of Ca^{2+} ions, the outer surface of the membrane bears a net negative charge, setting a local negative surface potential. On the other hand, we cannot discard the presence of discrete intrinsic K^+ permeability in BBMVs. In our experimental conditions, the presence of 2 mM Ca^{2+} effectively shielded the charged surface, reducing considerably the effects of surface potential changes, and decreased endogenous permeability (Fig. 2).

We show here that a steady-state condition can be established in the presence of 2 mM $CaCl_2$ under appropriate concentration of cyanine and valinomycin. A low concentration of the cyanine dye was recommended to avoid high concentration of the charged dye inside the vesicles and depolarization of the vesicles. Also, a low valinomycin concentration was recommended to induce K^+ permeability without drastically modifying the chemical gradient. In these steady-state conditions, estimations of E_R

can be obtained using the K^+-specific ionophore valinomycin. A linear response on the plot of changes in fluorescence versus the E_K, as predicted by the Nernst equation, was observed. The estimation of the BBMV E_R value performed when different monovalent cations (Na^+, TMA^+ or $NMDG^+$) were present in the external solution showed no differences, indicating that isolated BBMVs show poor permeability to these cations.

The influence of osmolarity and ionic strength during the E_R estimation was analyzed. The changes of these parameters were observed in the presence of 2 mM Ca^{2+}. Under these conditions, no statistical differences in E_R and in relative K^+ permeability were observed (Fig. 3A, B). A previous report from Kirouac et al. [15] suggested that osmolarity and ionic strength have a dramatic effect on $diSC_3(5)$ dye sensibility and on the estimations of changes in membrane potential. It is important to mention that these authors did not take into account the effects that pH and ionic strength have on the surface potential. Also, they used a high valinomycin concentration (7.5 μM) for 1-h incubation, which most probably affected the assay by dissipating the K^+ gradient. We found that if the surface potential is shielded correctly and the endogenous permeability is reduced, the changes in osmolarity or ionic strength did not affect the estimations of membrane potential performed with this fluorescent dye (Fig. 3).

Different reports have demonstrated the capacity of Cry toxins to induce pore formation in midgut tissues and insect midgut BBMVs using different experimental strategies (for review, see Schwartz & Laprade [23]). Cry toxin channels are poorly selective, transporting different ions and solutes of higher size including sugars and amino acids [2, 23–26]. However, all these studies were done only with Cry toxins in their monomeric state [2, 23–26]. Previously, we showed that the oligomeric structure of Cry1Ab is able to interact with synthetic membranes, in contrast to the monomeric Cry1Ab structure, which has marginal interaction with the liposomes [7]. The pore-formation activity of the Cry1Ab oligomeric structure analyzed in synthetic planar lipid bilayers revealed different kinetic characteristics from the monomeric Cry1Ab toxin [7]. The responses of pure oligomer preparations were observed at much lower toxin concentrations than the monomeric toxin, and the kinetics were different since oligomeric Cry1Ab showed stable channels that had a high open probability, in contrast to the monomeric toxin, which showed an unstable opening pattern [7].

In the present work, we reported that oligomeric Cry1Ab at 2.5 nM has higher activity compared with monomeric Cry1Ab toxin in BBMVs where receptors are present and showed that pore formation was dose-dependent (Fig. 4). These data are in agreement with previous reports which showed that the oligomeric structure of Cry1Ab toxin is membrane insertion-competent and demonstrates higher pore-formation activity than the monomeric toxin [5, 7, 9]. It is important to mention that the increased pore-formation activity of the oligomeric structure of the Cry1A toxins could also be due to the increased affinity of the oligomers to the membrane and to the APN receptor [4] and not only because the monomeric structure of these toxins is less active.

Further work is necessary to understand the functional characterization of these two Cry toxin structures.

M. sexta is sensitive to several Cry toxins: Cry1Aa, Cry1Ab, Cry1Ca, Cry1Da, Cry1Ea and Cry1Fa (Table 1). Protoxin samples from these toxins were activated with *M. sexta* BBMVs, showing formation of an oligomeric structure (Fig. 5B), in contrast to the same toxins activated with trypsin, where only monomeric structures were found (Fig. 5A). All samples of Cry1 toxins that contain a mixture of oligomeric and monomeric structures induced higher K^+ permeability than samples containing only monomeric toxin (Fig. 5C). These data support the hypothesis that the oligomeric structure of Cry toxins is the intermediate responsible for its insertion into the membrane. Undoubtedly, more efforts are necessary to improve our understanding of the differences in the mechanism of action of each of these Cry1 toxins as well as for identifying their specific receptors in *M. sexta* midgut membranes.

The membrane potential-sensitive fluorescent probe $diSC_3(5)$ is a useful and reliable tool for analyzing pore-formation activity of Cry toxins in natural or artificial membranes. This technique can be used as a screening assay for new toxins and for novel engineered Cry toxins.

Our thanks to Lizbeth Cabrera for technical assistance and CONACyT J44962Q for financial support.

References

1. Maagd, R.A., Bravo, A., Crickmore, N. 2001. How *Bacillus thuringiensis* has evolved specific toxins to colonize the insect world. *Trends Genet.* **17:**193–199
2. Schnepf, E., Crickmore, N., Rie, J., Lereclus, D., Baum, J., Feitelson, J., Zeigler, D.R., Dean, D.H. 1998. *Bacillus thuringiensis* and its pesticidal crystal proteins. *Microbiol. Mol. Biol. Rev.* **62:**775–806
3. Bravo, A., Jansens, S., Peferoen, M. 1992. Immunocytochemical localization of *Bacillus thuringiensis* insecticidal crystal proteins in intoxicated insects. *J. Invertebr. Pathol.* **60:**237–246
4. Bravo, A., Gómez, I., Conde, J., Muñoz-Garay, C., Sánchez, J., Miranda, R., Zhuang, M., Gill, S.S., Soberón, M. 2004. Oligomerization triggers binding of a *Bacillus thuringiensis* Cry1Ab pore-forming toxin to aminopeptidase N receptor leading to insertion into membrane microdomains. *Biochim. Biophys. Acta.* **1667:**38–46

5. Gómez, I., Sánchez, J., Miranda, R., Bravo, A., Soberon, M. 2002. Cadherin-like receptor binding facilitates proteolytic cleavage of helix α-1 in domain I and oligomer pre-pore formation of *Bacillus thuringiensis* Cry1Ab toxin. *FEBS Lett*. **513:**242–246
6. Zhuang, M., Oltean, D.I., Gomez, I., Pullikuth, A.K., Soberon, M., Bravo, A., Gill, S.S. 2002. *Heliothis virescens* and *Manduca sexta* lipid rafts are involved in Cry1A toxin binding to the midgut epithelium and subsequent pore formation. *J. Biol. Chem*. **277:**13863–13872
7. Rausell, C., Muñoz-Garay, C., Miranda-CassoLuengo, R., Gómez, I., Rudiño-Piñera, E., Soberón, M., Bravo, A. 2004. Tryptophan spectroscopy studies and black lipid bilayer analysis indicate that the oligomeric structure of Cry1Ab toxin from *Bacillus thuringiensis* is the membrane-insertion intermediate. *Biochemistry* **43:**166–174
8. Rausell, C., Pardo-López, L., Sánchez, J., Muñoz-Garay, C., Morera, C., Soberón, M., Bravo, A. 2004. Unfolding events in the water-soluble monomeric Cry1Ab toxin during transition to oligomeric pre-pore and membrane inserted pore channel. *J. Biol. Chem*. **279:**55168–55175
9. Rausell, C., García-Robles, I., Sánchez, J., Muñoz-Garay, C., Martínez-Ramírez, A.C., Real, M.D., Bravo, A. 2004. Role of toxin activation on binding and pore formation activity of the *Bacillus thuringiensis* Cry3 toxins in membranes of *Leptinotarsa decemlineata* [Say]. *Biochem. Biophys. Acta*. **1660:**99–105
10. Lorence, A., Darszon, A., Díaz, C., Liévano, A., Quintero, R., Bravo, A. 1995. δ-Endotoxins induce cation channels in *Spodoptera frugiperda* brush border membranes in suspension and in planar lipid bilayers. *FEBS Lett*. **360:**217–222
11. Lorence A., Darszon A., Bravo A. 1997. The pore formation activity of *Bacillus thuringiensis* Cry1Ac toxin on *Trichoplusia ni* membranes depends on the presence of aminopeptidase N. FEBS Lett. 414:303–307
12. Bashford, C.L., Smith, J.C. 1979. The use of optical probes to monitor membrane potential. *Methods Enzymol*. **55:**569–586
13. Waggoner, A. 1976. Optical probes of membrane potential. *J. Membr. Biol*. **27:**317–334
14. Cabrini, G., Verkman, A.S. 1986. Localization of cyanine dye binding to brush border membranes by quenching of n-(9-anthroyloxy) fatty acid probes. *Biochim. Biophys. Acta*. **862:**285–293
15. Kirouac, M., Vachon, V., Rivest, S., Schwartz, J-L., Laprade, R. 2003. Analysis of the properties of *Bacillus thuringiensis* insecticidal toxins using a potential-sensitive fluorescent probe. *J. Membr. Biol*. **196:**51–59
16. Bravo, A., Miranda, R., Gómez, I., Soberon, M. 2002. Pore formation activity of Cry toxins from *Bacillus thuringiensis* in an improved membrane preparation from *Manduca sexta* midgut cell microvilli. *Biochem. Biophys. Acta*. **1562:**63–69
17. Harlow, E., Lane, D. 1988. Antibodies. A Laboratory Manual. Cold Spring Harbor Laboratory, Cold Spring Harbor, NY
18. Gómez, I., Oltean, D.L, Gill, S.S., Bravo, A., Soberón, M. 2001. Mapping the epitope in cadherin-like receptors involved in *Bacillus thuringiensis* Cry1A toxin interaction using phage display. *J. Biol. Chem*. **276:**28906–28912
19. Güereca, L., Bravo, A. 1999. The oligomeric state of *Bacillus thuringiensis* Cry toxins in solution. *Biochim. Biophys. Acta*. **1429:**342–350
20. Höfte, H., Grave, H., Seurinck, J., Jansens, S., Mahillon, J., Ampe, C., Vandekerckhove, J., Vanderbruggen, H., VanMontagu, M., Zabeau, M., Vaek, M. 1986. Structural and functional analysis of a cloned delta endotoxin of *Bacillus thuringiensis* berliner 1715. *Eur. J. Biochem*. **161:**273–280
21. Hille, B. 1992. Chapter 16 structure and function In: B. Hille, editor. Ionic Channels of Excitable Membranes, pp. 427–464. Sinauer Associates, Suderland, MA
22. Watts A., van Gorkom C.M. 1991. Surface organization of lipid bilayers. In: P. Yeagle, editor. The Structure of Biological Membranes. CRC Press, New York
23. Schwartz J.L., Laprade R. 2000. Membrane permeabilization by *Bacillus thuringiensis* toxins: Protein insertion and pore formation. In: J. F. Charles, A. Deleeluse, C. Nielsen-LeRoux et al., editors. Entomopathogenic Bacteria: From Laboratory to Field Application. Kluwer Academic, Amsterdam, Dordrecht, The Netherlands, pp. 199–217
24. Carroll, J., Ellar, D.J. 1993. An analysis of *Bacillus thuringiensis* δ-endotoxin action on insect midgut membrane permeability using a light scattering assay. *Eur. J. Biochem*. **214:**771–778
25. Carroll, J., Ellar, D.J. 1997. Analysis of the large aqueous pores produced by *Bacillus thuringiensis* protein insecticide in *Manduca sexta* midgut brush border membrane vesicles. *Eur. J. Biochem*. **245:**797–804
26. Tran, B.L., Vachon, V., Shwartz, J.L., Laprade, R. 2001. Differential effects on the pore formation properties of *Bacillus thuringiensis* insecticidal crystal proteins. *Appl. Environ. Microbiol*. **67:**4488–4494